JACS
JOURNAL OF THE AMERICAN CHEMICAL SOCIETY

Article

pubs.acs.org/JACS

Examining Photoinduced Energy Transfer in *Pseudomonas aeruginosa* Azurin

Peter H. Tobin[†] and Corey J. Wilson*[,†,‡,§]

[†]Department of Chemical and Environmental Engineering, [‡]Department of Biomedical Engineering, and [§]Department of Molecular Biophysics and Biochemistry, Yale University, New Haven, Connecticut 06520-8286, United States

Supporting Information

ABSTRACT: *Pseudomonas aeruginosa* azurin has been an important model system for investigating fundamental electron transfer (EleT) in proteins. Early pioneering studies used ruthenium photosensitizers to induce EleT in azurin and this experimental data continues to be used to develop theories for EleT mediated through a protein matrix. In this study we show that putative EleT rates in the *P. aeruginosa* azurin model system, measured via photoinduced methods, can also be explained by an alternate energy transfer (EngT) mechanism. Investigation of EngT in azurin, conducted in this study, isolates and resolves confounding phenomena—i.e., zinc contamination and excited state emission—that can lead to erroneous kinetic assignments. Here we employ two azurin photosensitizer systems, the previously reported Ru(2,2′-bipyridine)$_2$(imidazole) and an unreported phototrigger, Ru(bpy)$_2$(phen-IA), Ru(2,2′-bipyridine)$_2$(5-iodoacetamido-1,10-phenanthroline), that has a longer lifetime, to better resolve convoluted kinetic observations and allow us to draw clear distinctions between photoinduced EngT and EleT. Extensive metal analysis, in addition to electrochemical and photochemical (photoinduced transfer) measurements, suggests Zn-metalated azurin contamination can result in a biexponential reaction, which can be mistaken for EleT. Namely, upon photoinduction, the observed slow phase is exclusively the contribution from Zn-metalated azurin, not EleT, whereas the fast phase is the result of EngT between the photosensitizer and the Cu-site, rather than simple excited-state decay of the phototrigger.

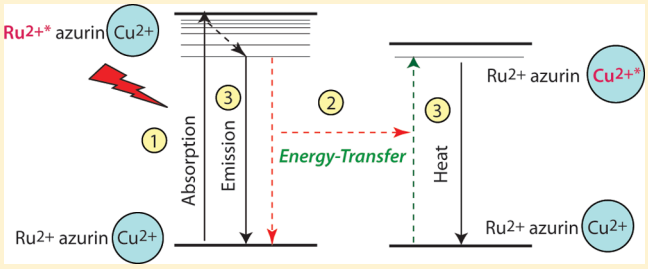

INTRODUCTION

Electron transfer (EleT) and energy transfer (EngT) are of critical importance in biology due to their fundamental roles in bioenergetic processes such as photosynthesis, in addition to various biological systems.[1−7] The two transfer processes are important because they can be used to quench electronically excited states and to sensitize other species. From a quantum mechanical viewpoint, EleT and EngT processes can be viewed as radiationless transitions between different, weakly interacting electronic states.[8,9] The key distinctions between photoinduced EleT and EngT are the mechanism of electronic transition (Scheme 1) and theoretical distance limits of transfer. To keep EleT rates within the millisecond to microsecond range the effective distance limit is ∼20 Å if the reaction is facilitated without a "hopping intermediate",[10−12] whereas EngT processes can occur at distances up to 70 Å.[13,14]

Several experimental methods have been developed to measure the rate of EleT within various protein systems;[15,16] however, experimental assessment of related EngT processes has lagged significantly for these same systems. The dominant method for measuring EleT within proteins is achieved by way of intramolecular photochemical induction.[12,15,17−19] The advantage of photochemically induced EleT over other methods[16,20−23] is the ability to use site-specific covalent attachment of a tunable photosensitizer (phototrigger) to the

Scheme 1. Comparison and Contrast of Electron Transfer and Energy Transfer Mechanisms

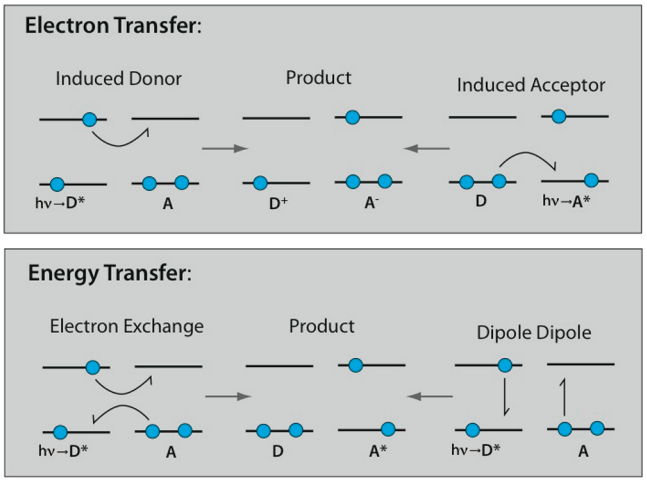

Received: April 30, 2013
Revised: December 3, 2013
Published: January 14, 2014

surface of a EleT protein, which allows for experimental control over the EleT pathway, distance, and driving force for the reaction.[15]

Pseudomonas aeruginosa azurin is a small (14 kDa), soluble blue copper protein with a β-sandwich fold which has become one of the key model systems for investigating intramolecular EleT in proteins.[12,15−19,24] The blue copper site in azurin has a strong absorbance peak at 625 nm in the Cu^{2+} state, which is absent in the Cu^{+} state. The transient change in absorbance between redox states (mediated by activation of a surface-attached photosensitizer) is the key observable in most studies of intramolecular EleT in azurin (see Scheme 2). Accordingly,

Scheme 2. Original Kinetic Mechanisms Proposed in Early Pioneering Studies[17,31] of Ruthenium Photosensitizer-Mediated Electron Transfer in Azurin[a]

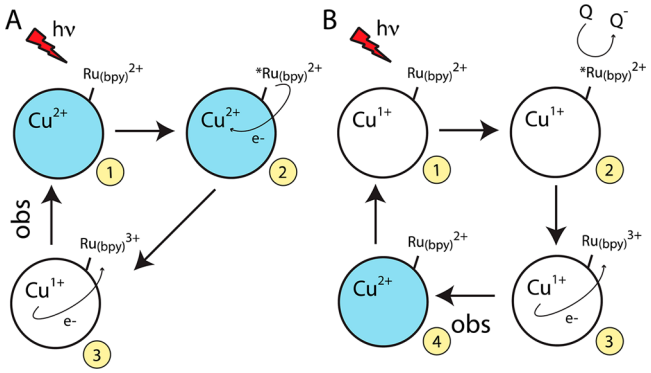

[a](A) Photoinduced reaction scheme: (1) laser excitation at 480 nm of Ru^{2+}-azurin/Cu^{2+} results in the formation of the Ru^{2+}*-azurin/Cu^{2+} excited state, (2) forward electron transfer (too fast to be observed with the original experimental setup) results in the formation of Ru^{3+}-azurin/Cu^{+}, and (3) back electron transfer from Cu^{+} to Ru^{3+} yields a return to the ground state and is the putative observable measured via transient absorption kinetics. (B) Flash-quench reaction scheme: (1) laser excitation at 480 nm of Ru^{2+}-azurin/Cu^{+} results in the formation of the Ru^{2+}*-azurin/Cu^{+} excited state, (2) oxidative quenching by $Ru(NH_3)_6^{3+}$ yields Ru^{3+}-azurin/Cu^{+}, (3) back electron-transfer from Cu^{+} to Ru^{3+} yields Ru^{2+}-azurin/Cu^{2+} and is the putative observable measured via transient absorption kinetics, and (4) on a longer time scale the reduced quencher $Ru(NH_3)_6^{2+}$ reduces Cu^{2+}, re-forming the initial Ru^{2+}-azurin/Cu^{+}.

these elegant experimental approaches have been used to measure the rates of charge transfer in the azurin model system, and flash-quench methods (Scheme 2B) have been used to create extensive timetables of EleT—i.e., distance- and pathway-dependent rates of charge transfer—in the azurin and cytochrome *c* model systems.[15] In addition, the two photochemical methods[25] were used to determine the reorganization energy for the azurin Cu site. In turn, these data have been used to parametrize the semiclassical (Marcus) model of electron transfer and have been leveraged to expand our understanding of electronic coupling, including pathway dynamics.[26,27] Eventually, this knowledge will aid in the development of explicit protein design models and scoring functions for engineering synthetic bioenergetic and biocatalytic processes.

A variety of photosensitizers have been used in attempts to measure photoinduced intramolecular EleT in azurin—e.g., pentaammineruthenium,[24] $Ru(bpy)_2Im$,[17,25] $Re(CO)_3(phen)$,[28] Os(trpy)(bpy),[25] and thioureidopyrenetrisulfonate (TUPS).[29] Additionally, experiments utilizing pulse radiolysis have also been conducted, to measure intramolecular charge-transfer rates.[16] Unfortunately, for the photoinduced method, there are a few inconsistencies as to the assignment of the EleT rate to the observed experimental data, such as whether the observed transients are due solely to EleT and can be fit with a single exponential model[25,30] or whether the observed transients must be decomposed into a double exponential model with emission decay of the photosensitizer corresponding to a second rate.[31−33] Accordingly, controversies remain with regard to the exact nature (mechanism) of biological EleT—e.g., the role of amino acid composition in electronic coupling pathways.[34] We believe some of the inconsistencies arise from our inability to clearly distinguish between EleT and EngT in these systems. Accordingly, in this study we present methodology for measuring EngT that leverages techniques initially developed to measure photoinduced EleT. In addition, we resolve confounding kinetic phenomena associated with Zn contamination in the model system *P. aeruginosa* azurin that can result in erroneous kinetic assignments when measuring EleT via photoinduction.

MATERIALS AND METHODS

Variant Construction, Protein Expression, and Purification. A pUG4 (pUC18-based) vector containing the wild-type *P. aeruginosa* azurin gene[35] was used as a template, and variants (H83C, K92C, H83Q T124C, T30C, H83Q Q107C, D98C, E104C, H83Q K92H, H83Q T124H, H83Q T126H, and H83Q Q107H) were constructed using the SOEing technique[36] with oligos purchased from Sigma. All variant sequences were verified by DNA sequencing at the Yale W.M. Keck Biotechnology Resource Laboratory. Azurin variants were purified from *E. coli* BL21 cells transformed with plasmid pUG4 containing the appropriate *P. aeruginosa* azurin gene (wild-type or mutant) in a manner similar to earlier reports.[37] First, 6 L of LB medium per variant (1 L per 2 L flask) plus 100 μg/mL ampicillin was inoculated 2 mL/L from a 7 h, 14 mL LB ampicillin culture started from a single colony. Four hours after inoculation, azurin expression was induced by the addition of 1 mL/L 0.5 M IPTG and 1 mL/L 0.1 M $CuSO_4$ at the same time. Cells were grown for 12−14 h at 37 °C with 250 rpm shaking and then collected by centrifugation (4000 rpm for 15 min). Cell paste was resuspended in 20% (w/v) sucrose, 300 mM Tris-HCl, and 1 mM EDTA buffer, broken in a french press (Avestin EmulsiFlex-C5), and centrifuged (10 000 rpm for 30 min). Next, 0.1 M $CuSO_4$ to a concentration of 0.01 M, and 0.5 M NH_4OAc pH 4.0 to a concentration of 0.05 M, were added to the supernatant, and the pH was adjusted to 4.0 with concentrated HOAc. Precipitated proteins were removed by centrifugation (10 000 rpm for 30 min). The supernatant was dialyzed overnight into 50 mM NH_4OAc pH 4.0, and centrifuged again (10 000 rpm for 15 min) to remove additional precipitant. The 0.22 μm filtered supernatant was applied to a Highload 26/10 SP Sepharose column in an Akta HPLC system (GE) equilibrated with 50 mM NH_4OAc pH 4.0. Azurin was eluted with a 50 mM NH_4OAc pH gradient of 4.0−9.5. Blue fractions were pooled, concentrated (Amicon Ultra 10K MWCO), and applied to a Superdex 75 column (GE) equilibrated with 50 mM KP buffer pH 7.5. Monomeric fractions were retained (peak at 78 mL), and oligomeric fractions (more prevalent in Cys mutants due to intermolecular disulfide formation) were discarded. The purified azurin was judged pure by SDS-PAGE, and the 628/280 nm absorbance ratio was 0.35−0.45 at this stage.

Metalization and Photosensitizer Labeling. Apo-azurin was formed by dialysis against KCN.[37−39] Up to 40 mL of 100 μM heteroazurin was dialyzed against 1 L of fresh 0.5 M KCN|100 mM Tris pH 8.5 for two 4 h exchanges, followed by three exchanges into 50 mM KP buffer pH 7.5 for 1 h, overnight, and then 1 h. Cu or Zn loading was performed by dialysis overnight into 200 μM $CuSO_4$ or $ZnSO_4$ in 100 mM Tris pH 7.5, followed by several rounds of dialysis

dx.doi.org/10.1021/ja412308r | J. Am. Chem. Soc. 2014, 136, 1793−1802

to remove excess metal. $Ru(bpy)_2CO_3$ was synthesized according to a literature method.[40] Sodium carbonate was purchased from Sigma, and $Ru(bpy)_2Cl_2$ from Strem. Azurin was labeled with Ru(bpy)$_2$(imidazole) at His83 (WT), H92 (H83Q K92H), H124 (H83Q T124H), H126 (H83Q T126H), and H107 (H83Q Q107H) following a literature procedure.[41] Ru(bpy)$_2$(5-iodoacetamido-1,10-phenanthroline) was synthesized according to a literature method.[42] 5-Amino-1,10-phenanthroline and iodoacetic anhydride were purchased from Sigma. Azurin cysteine mutants H83C, K92C, H83Q T124C, T30C, H83Q Q107C, D98C, and E104C were labeled with thiol-reactive Ru(2,2′-bipyridine)$_2$(5-iodoacetamido-1,10-phenanthroline) [Ru(bpy)$_2$(phen-IA)] in a manner similar to a literature method.[42] A 10-fold molar excess of $[Ru(bpy)_2(phen\text{-}IA)](PF_6)_2$ was added in DMF to fresh H83C apo-azurin in 100 mM phosphate buffer pH 7.1 and allowed to react overnight at 4 °C in the dark. Ru(bpy)$_2$(phen-IA)-labeled apo-azurin was metal-loaded by dialysis as described above. Both Ru(bpy)$_2$Im- and Ru(bpy)$_2$(phen-IA)-labeled azurin variants were purified by cation exchange chromatography using a linear gradient from 25 to 600 mM NaOAc pH 4.5,[41] on a GE Akta Purifier system with a Highload 26/10 SP Sepharose column to remove unlabeled protein. Finally, gel filtration and buffer exchange into 50 mM KP pH 7.5 were performed using a Superdex 75 column.

Equilibrium Unfolding. Guanidine hydrochloride (GuHCl)-induced equilibrium unfolding was performed in 100 mM phosphate pH 7.0 at 25 °C and observed using fluorescence (excitation at 285 nm; emission at 308 nm) and far-UV circular dichrosim detection (220 nm for the heteroazurin sample, due to quenching of the native tryptophan fluorescence in the presence of Cu)[43] on an Applied Photophysics Chirascan spectrophotometer, as described previously.[37] The 8 M GuHCl used was purchased from Sigma. Samples were incubated for 2 h before measurements. The equilibrium unfolding curves were analyzed using two-state and three-state models.[37,44]

Zinc Analysis. Zinc content was measured using a Thermo Scientific Element XR inductively coupled plasma mass spectrometer, similar to the method used in ref 45. All sample preparation was conducted in a Class 10 trace-metal-free clean room, Geology and Geophysics Department, Yale University. All volumetric additions of sample components and dilutions were verified gravimetrically to ±0.001 mg on a Mettler Toledo XP26 analytical balance. A 40 μL aliquot of each sample (1 mg/mL azurin, based on ε = 9000 M^{-1} cm^{-1} at 280 nm in 100 mM KP pH 7.0, washed with EDTA prior to metal analysis) was pipetted volumetrically into a 3 mL acid-cleaned Teflon beaker and dried overnight on a hot plate at 95 °C. The dried samples were dissolved in 600 μL of 8 N ultrapure HNO_3 plus 200 μL of ultrapure H_2O_2 (both SEASTAR Baseline brand with metals under 10 ppt) and dried overnight on a hot plate at 95 °C, and this step was repeated a second time the following day. The dried samples were then dissolved in 3.8 mL of 5% (w/w) HNO_3 (SEASTAR Baseline) with 2 ppb ^{155}In (SPEX Certiprep) for analysis. Prior to HNO_3 and H_2O_2 digestion, Cu-metalated and Zn-metalated azurin samples of equal 280 nm absorbance (measured with a Thermo Scientific Genesys 10S UV−vis spectrophotometer) were mixed to create samples with 75%, 50%, and 25% Zn-metalated azurin. Three replicates of each sample type (blank, Zn-metalated azurin, 75% Zn-metalated azurin, 50% Zn-metalated azurin, 25% Zn-metalated azurin, and Cu-metalated azurin) were analyzed. Calibration was achieved by standard addition of certified standard reference material (Zn standard, SPEX Certiprep) in the range 0−100 ng/g, 20 ng/g step, to apo-azurin samples (6-point calibration). ^{155}In at 2 ppb was used as an internal standard to correct for instrumental drift and was included in all samples. ^{66}Zn, ^{67}Zn, and ^{68}Zn were measured, and the standard addition calibration was linear with R^2 > 0.999 for all three isotopes.

Electrochemistry. Azurin oxidation and reduction peak potentials, E_p^{ox} and E_p^{red}, were measured via cyclic voltammetry using a CH Instruments model 660 electrochemical workstation and model CHI222 glass cell equipped with a glassy carbon working electrode, platinum wire counter electrode, and an Ag/AgCl (1 M KCl) reference electrode. Four-milliliter volumes of 0.2 μm filtered 100 μM samples of photosensitizer-labeled azurin in 50 mM KP pH 7.5 were used for all experiments under ambient atmosphere at room temperature (21 °C), with a scan rate of 0.01 V/s, and repeatable quasireversible voltammograms were obtained. Reported midpoint potentials (E_m) were calculated according to eq 1:

$$E_m = \frac{E_p^{ox} + E_p^{red}}{2} \quad (1)$$

Mixed concentrations of Cu- and Zn-loaded azurin were obtained by mixing appropriate volumes of 100 μM Cu-loaded and 100 μM Zn-loaded azurin. In this method (inspired by Sykes's work[46] with plastocyanin using $[\text{-}Ru(NH_3)_5]^{3+/2+}$ attached at His59 and Zanello's[47] descriptions of protein interactions with negatively charged glassy carbon electrodes), the 2+ charge on the attached Ru photosensitizer acts as a mediator to allow interaction between negatively charged azurin (isoelectric point <6) at pH 7.5 and the negatively charged glassy carbon working electrode. Under equivalent conditions at pH 7.5, unlabeled azurin yields less reversible and much smaller amplitude oxidation and reduction peaks.

Photochemistry. Kinetic measurements were conducted using an Applied Photophysics LKS 60 ns laser flash photolysis spectrometer combined with a Newport Spectra-Physics Nd:YAG-pumped optical parametric oscillator and UV scan generator. For kinetic experiments Ru(bpy)$_2$(phen-IA)-azurin concentration was 30 μM based on ε = 16 600 M^{-1} cm^{-1} at 450 nm for Ru(bpy)$_2$(phen-IA)[42] and 30−120 μM based on ε = 10 000 M^{-1} cm^{-1} at 490 nm for Ru(bpy)$_2$Im-azurin.[41] Use of 120 μM Ru(bpy)$_2$Im-azurin gave higher amplitude signals but otherwise equivalent results. Protein solutions were bubbled with argon for 10 min in a cuvette which was then sealed prior to measurements. EDTA wash was done prior to measurements to remove any adventitious metals. λ_{ex} was set at 450 nm for Ru(bpy)$_2$(phen-IA) and 480 or 490 nm for Ru(bpy)$_2$Im-azurin and confirmed spectroscopically. Excitation at 490 nm for Ru(bpy)$_2$Im-azurin gave higher amplitude signals but otherwise equivalent results. Laser power was measured with a Newport laser power meter and adjusted to 2 mJ/pulse to match previous work.[25] Transient emission and absorption were monitored at 625 nm and controlled by two monochromators, one between the xenon flash lamp and the sample and the other between the sample and the detector (see Figure S10). Each measurement was the average of eight laser shots, with a 1 s delay between shots. Reported rates are the average of three 8-shot averages. Reported photosensitizer lifetimes ($\tau = 1/k_{avg}$) are the inverse of the average zinc-metalated transient emission rates at 625 nm for all azurin variants labeled with that photosensitizer. Kinetic data were fit to single exponential and biexponential models using Kaleidagraph, and global fitting was performed in Igor Pro. Data for transient absorption experiments with mixed percentages of Cu-metalated and Zn-metalated samples (7−54% Zn content) for Ru(bpy)$_2$Im(His^{83})-azurin were globally fit to eq 2, yielding a global k_1 and k_2, and individual coefficients C, A_1, and A_2, and this method was repeated for transient emission data and for equivalent Ru(bpy)$_2$(phen-IA)(Cys^{83}) azurin data.

$$Y(t) = C + A_1\exp(-k_1 t) + A_2\exp(-k_2 t) \quad (2)$$

RESULTS AND DISCUSSION

Preparation of Cu-Azurin and Quantification of Cu/Zn-Metalization. We recombinantly express *P. aeruginosa* azurin in *E. coli* using standard laboratory methods.[35,37,39,48] In our hands, protein enriched via cation exchange (see Methods and Materials) contains 27−44% Zn-metalated azurin (see Table 1). In practice, two methods have been used to produce Cu-azurin for photochemistry measurements: (i) enrichment of apo-azurin via anion exchange, followed by Cu metalization,[41,49,50] and (ii) Cu remetalization of apoprotein produced using a strong chelating agent.[39] Our heteroazurin samples were nearly devoid of apo-azurin; accordingly, we used the latter (chelation) approach to produce uniform Cu-azurin and Zn-azurin (control) samples. Namely, we dialyzed

Table 1. 628/280 nm Absorbance Ratio vs %Zn from ICP-MS[a]

azurin forms, wild-type	GuHCl unfolding midpoints (M)	628/280 nm absorbance ratio	Zn content (%)
hetero-azurin	3.2	0.40 ± 0.01	36
partial Zn-azurin[b]	1.85/3.2[d]	0.00	25
apo-azurin[c]	1.85	0.00	7
Zn-azurin	3.2	0.00	100
Cu-azurin	3.3	0.56 ± 0.01	7

[a]Correlation given in Figure S2. [b]Holo-azurin after 2 h exposure to KCN; also see Figure S1. [c]Holo-azurin after 8 h exposure to KCN; also see Figure S1. [d]First midpoint/second midpoint.

heteroazurin (i.e., post cation exchange) against KCN[37−39] to remove mixed metals from the heterogeneous azurin sample, producing a homogeneous apo-azurin sample. To quantify azurin demetalization, protein stability analysis was conducted via equilibrium unfolding experiments, as the amount of Zn removal cannot be determined spectroscopically (Figure S1). Zn-metalated azurin is 29 kJ mol^{-1} more stable than apo-azurin;[37,48] accordingly, partially Zn-metalated azurin presents biphasic transitions (though spectroscopically indistinguishable from the apoprotein, also see Table 1 and Figure S1), while apo-azurin shows a single transition. In turn, apo-azurin was remetalated with either Cu or Zn to achieve monometalation, using a simple dialysis against excess metal in the dialysate solution. Cu-azurin produced in this manner had a 628/280 nm absorbance ratio of 0.56 ± 0.01, similar to earlier reports, which were considered pure Cu-azurin.[33,38,50]

To better quantify any Zn content in our samples, we conducted inductively coupled plasma mass spectrometry (ICP-MS) on apo-azurin, Cu-metalated, and Zn-metalated protein (see Table 1). The average Zn content of three replicates of Zn-metalated azurin tested was 47.6 ppb, which is consistent with 100% Zn occupancy, considering an uncertainty of up to 10% in the ε_{280} (based on the 280 nm absorbance and quantity of azurin solution in each sample for an ε_{280} of 9000 M^{-1} cm^{-1},[50] 49.0 ppb would be expected, and for an ε_{280} of 9800 M^{-1} cm^{-1},[38] 45.5 pbb would be expected for a 1:1 azurin to Zn^{2+} stoichiometric ratio). The average Zn content of three replicates of apo-azurin was 3.1 ppb, and for Cu-metalated azurin 3.5 ppb, yielding approximately 7% Zn content for both our apo and Cu-metalated samples. Notably, 7% Zn contamination is consistent with an earlier report[50] in which Cu-azurin was prepared by way of metalated apoprotein isolated via anion exchange chromatography. A comparison of the 628/280 nm absorbance ratio for mixed Cu-metalated and Zn-metalated samples and the ICP-MS measured Zn content yields an extrapolated 628/280 ratio of 0.60 for Zn-free azurin (Figure S2). The voltammograms in Figure S3 demonstrate that Cu-metalated azurin prepared via Cu remetalization is redox active, with an observed potential of 68 ± 1 mV vs Ag/AgCl, on par with values reported in previous studies.[51−53]

Photochemical Characterization of Metalated Azurin. Zn-metalated protein reference experiments were not reported in any of the earlier accounts of $Ru(bpy)_2Im$-labeled photoinduced EleT in azurin,[25,30,31,33] and they were only tentatively explored in the most recent account.[32] To investigate the influence of Zn-azurin contamination on the rate of charge transfer, Cu-metalated (i.e., 93% Cu/7% Zn) and 100% Zn-metalated azurin were subjected to photochemical characterization to measure putative EleT rates via photoinduction (see Scheme 2A) under conditions closely matching those used by earlier investigators (also see Methods and Materials).[25,31,32] Namely, previous reports of photoinduced experiments for $Ru(bpy)_2Im$-labeled azurin involved an excitation of $Ru(bpy)_2Im$ at 480−490 nm, followed by monitoring of transient absorbance (i.e., Cu^+ to Cu^{2+}) in the range of 625−632 nm.[25,30−33] Under these conditions using azurin labeled with $Ru(bpy)_2Im$ (0.11 μs lifetime) or $Ru(bpy)_2$(phen-IA) (1.7 μs lifetime) at amino acid position 83, we also observe an instantaneous drop in absorbance followed by a transient biexponential return to the pre-excitation baseline (see Figure 1; also see Supporting Information Figures S4A,B and S5A,B). This observation is in agreement with several previous reports,[31,33] which made the following assignments: the faster rate (k_1) was attributed to an excited-state decay of the photosensitizer (based on measurements of the protein-free model compound $Ru(bpy)_2Im_2$),[54] and the slower rate (k_2) was ascribed to back EleT (Ru^{3+}-azurin/Cu^+ to Ru^{2+}-azurin/Cu^{2+}) assuming a forward rate of electron transfer (Ru^{2+}*-azurin/Cu^{2+} to Ru^{3+}-azurin/Cu^+), which was described as too fast to be observed by the reported experimental setup, and this is the basis of Scheme 2A.[31] Moreover, our initial analysis for both

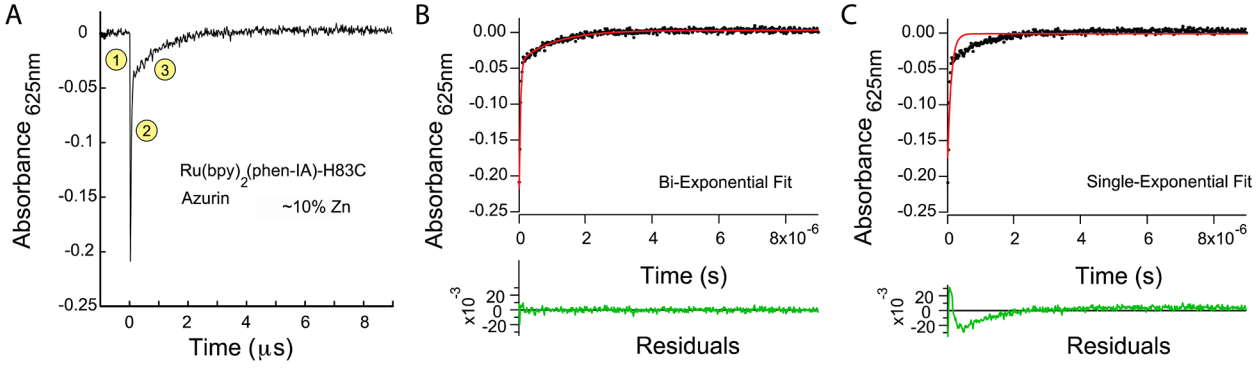

Figure 1. Kinetic assignments for $Ru(bpy)_2$(phen-IA)(Cys^{83}) photoinduction experiments. (A) Previous work with photochemistry experiments for $Ru(bpy)_2Im$-labeled azurin reported a biexponential reaction, observed at λ_{abs} = 625 nm via transient absorption kinetics, of oxidized protein excited at λ_{ex} = 480−490 nm. An instantaneous drop (1) at the Cu^{2+} absorption peak (in the range of 625−632 nm) was observed followed by a transient biexponential return (2 and 3) to the pre-excitation baseline. Initial analysis for both Cu-metalated $Ru(bpy)_2Im(His^{83})$ (see Figure S4A,B) and $Ru(bpy)_2$(phen-IA)(Cys^{83}) systems (also see Figure S5A,B) produced rates that are comparable to previously published rates. (B) Biexponential and (C) single exponential fits to 10% Zn $Ru(bpy)_2$(phen-IA)(Cys^{83}) azurin transient absorption data.

dx.doi.org/10.1021/ja412308r | J. Am. Chem. Soc. 2014, 136, 1793−1802

Cu-metalated Ru(bpy)$_2$Im(His^{83}) and Ru(bpy)$_2$(phen-IA)-(Cys^{83})systems produced rates that are comparable to previously published rates[25,31] (see Table 2).

Table 2. Transient Absorption Data for λ_{ex} = 490 nm, λ_{abs} = 625 nm[a]

azurin variants	Zn content (%)	k_1 ($\times 10^6$ s^{-1})	k_2 ($\times 10^6$ s^{-1})
Ru(bpy)$_2$(phen-IA) (Cys^{83})	7	33.2 ± 1.1	1.00 ± 0.08
Ru(bpy)$_2$(phen-IA) (Cys^{83})	100	0.646 ± 0.011	n/a
Ru(bpy)$_2$(phen-IA) (Cys^{83})	var.[b]	25.7 ± 0.4	0.801 ± 0.004
Ru(bpy)$_2$Im (His^{83})	7	21.6 ± 0.4	2.05 ± 0.61
Ru(bpy)$_2$Im (His^{83})	100	6.23 ± 0.14	n/a
Ru(bpy)$_2$Im (His^{83})	var.[b]	18.7 ± 0.4	5.91 ± 0.10

[a]Emission data given in Table S1. [b]Variable; rates determined via global analysis, using data collected in Figure 2.

Interestingly, experiments on mixed ratios of Cu/Zn-metalated protein demonstrate increased amplitudes for the slower rate k_2 and decreased amplitudes for the faster rate k_1 as the percentage of Zn-metalated protein is raised to 100% in both systems (see Figure 2; also see Figures S4 and S5). The

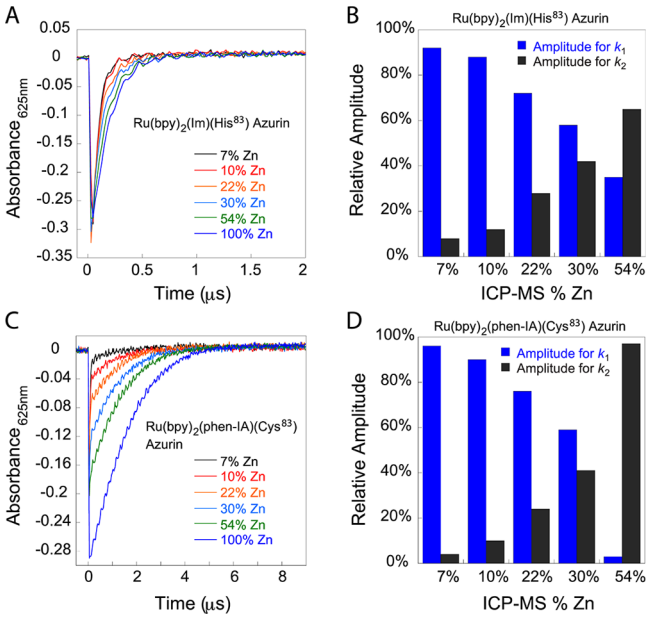

Figure 2. Transient absorption kinetics monitored at 625 nm using variable percentages of the Cu- and Zn-metalated forms: (A) Ru(bpy)$_2$Im(His^{83}) azurin and (C) Ru(bpy)$_2$(phen-IA)(Cys^{83}) azurin. (B) and (D) show relative amplitudes for the k_1 and k_2 rates from global fitting of the 7−54% Zn samples in (A) and (C), respectively. Individual kinetic traces and fits are given in Supporting Information, Figures S4 and S5.

homogeneous Zn-metalated azurin samples are best fit as a single-exponential decay with observed rates of k = 6.2 × 10^6 and 0.65 × 10^6 s^{-1} for Ru(bpy)$_2$Im(His^{83}) and Ru(bpy)$_2$(phen-IA)(Cys^{83}), respectively. Global biexponential fitting of transient absorption from un-mixed Cu-metalated azurin (7% Zn) and mixed samples with 10%, 22%, 30%, and 54% Zn yielded two distinct rates that correspond to the observed rate for homogeneous Cu-azurin (k_1) and Zn-azurin samples, respectively, i.e., for both Ru(bpy)$_2$Im(His^{83}) and Ru-(bpy)$_2$(phen-IA)(Cys^{83}) systems. Due to the longer lifetime (1.7 μs) of Ru(bpy)$_2$(phen-IA)(Cys^{83}), the effects of even small quantities of Zn-azurin contamination are more apparent (Figure 2C,D). The difference in the observed rates for the Cu-azurin slow phase and Zn-azurin single phase is likely due to missing kinetic amplitudes, which is resolved upon global analysis (see Table 2). Thus, the most reasonable supposition is that the slower rate (k_2) observed in the Cu-metalated (i.e., 7% Zn) sample is due to residual Zn-metalated azurin contamination, and not EleT.

Resolving the Observed Rates. What is the nature of the observed faster k_1 rates? Previous studies have suggested that EngT in addition to EleT could be responsible for some portion of the photoinduced transient absorption kinetics observed in cytochrome c[55] and azurin.[31] Accordingly, three events could contribute to the observed k_1 in the Cu-azurin system: (i) excited-state decay of the phototrigger, (ii) EleT, or (iii) EngT. However, the relative contributions of the three phenomena have not been carefully resolved for Ru(bpy)$_2$Im-labeled azurin. Is the observed (λ_{abs} = 625 nm) k_1 rate electron transfer? In principle, the rate of EleT has a distinct distance dependence.[15] Accordingly, to test Cu-azurin (i.e., Ru(bpy)$_2$Im-(His^X) and Ru(bpy)$_2$(phen-IA)(Cys^X) for EleT, we created several azurin variants in which the distance between the photosensitizer and Cu site varies and conducted transient absorption experiments via photoinduction (Scheme 2A), similar to the above (i.e., λ_{ex} = 490 nm and λ_{abs} = 625 nm; see Figure 3, Table 3, and Supporting Information Table S2). Interestingly, we observe nonlinear distance-dependent rates for k_1 in both systems, which is significantly faster than the putative rate versus distance relationship reported for EleT through a protein matrix. In addition, this result also eliminates

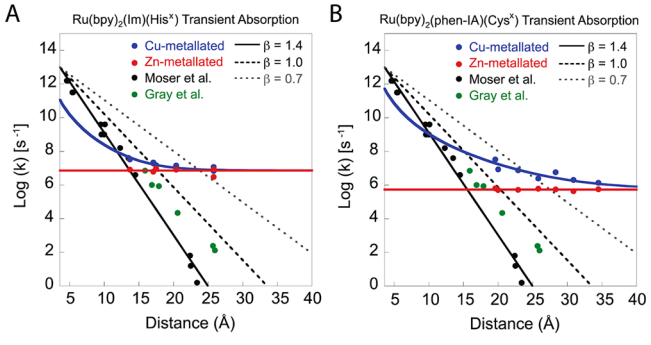

Figure 3. Transient absorption kinetics (625 nm) from this study plotted against the theoretical free-energy optimized rate versus distance relationship for EleT, and previous experimental data. Theoretical k_{EleT} (eq 3) rates with β = 1.4 (black solid line), 1.0 (gray dashed line), and 0.7 (gray dotted line), bacterial reaction centers (black circles),[57] and the Gray group's Ru(bpy)$_2$Im-labeled azurin flash quench data (green circles).[15] (A) Photoinduced Ru(2,2′-bipyridine)$_2$(imidazole) [Ru(bpy)$_2$(Im)]-labeled azurin: Cu-metalated (this study, blue circles) and Zn-metalated (this study, red circles). (**B**) Photoinduced Ru(bpy)$_2$(phen-IA)-labeled azurin: Cu-metalated (this study, blue circles) and Zn-metalated (this study, red circles). Red solid lines are the average Zn-metalated (unquenched) rates, k_D = 0.547 × 10^6 s^{-1} for Ru(bpy)$_2$(phen-IA)-labeled azurin and k_D = 7.29 × 10^6 s^{-1} for Ru(bpy)$_2$(Im)-labeled azurin. Blue solid lines are the best-fit EngT rate curves (k_{obs}, eq 7), yielding R_0 = 35.5 Å for Ru(bpy)$_2$(phen-IA)-labeled azurin and R_0 = 17.9 Å for Ru-(bpy)$_2$(Im)-labeled azurin. Also see Tables 3 and S2.

dx.doi.org/10.1021/ja412308r | J. Am. Chem. Soc. 2014, 136, 1793−1802

Table 3[a]

azurin variants Ru(bpy)$_2$(phen-IA)	d (Å)	k_1 ($\times 10^6$ s^{-1}) at 625 nm abs for 93% Cu[b]	k_1 ($\times 10^6$ s^{-1}) at 625 nm abs for 100% Zn
H83C	19.6	33.2 ± 1.1	0.646 ± 0.011
K92C	20.0	8.60 ± 0.07	0.504 ± 0.012
H83QT124C	22.9	7.53 ± 0.24	0.521 ± 0.010
T30C	25.8	2.47 ± 0.07	0.612 ± 0.006
H83Q Q107C	28.3	5.76 ± 0.03	0.549 ± 0.011
D98C	30.9	2.04 ± 0.01	0.434 ± 0.003
E104C	34.5	1.35 ± 0.06	0.566 ± 0.002

[a]Azurin variants Ru(bpy)$_2$Im given in Supporting Information, Table S2; also see Figure S9 and Table S3. [b]93% Cu/7% Zn.

excited-state decay of the phototrigger as a satisfactory explanation for the observed rate; i.e., the observed k_1 rate is not simply the result of phototrigger decay because a constant rate is not observed for Cu-metalated azurin samples. To further test this assertion, we measured the decay rates for Zn-azurin for both Ru(bpy)$_2$Im(His^X) and Ru(bpy)$_2$(phen-IA)-(Cys^X), which show constant rates and are independent of distance (Figure 3 and Table 3).

Considering the significant overlap between emission of the photosensitizers and absorption of Cu^{2+} azurin (see Figure 4A

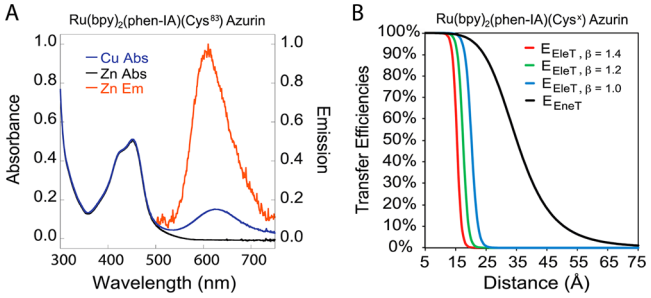

Figure 4. (A) UV/vis absorption spectra and normalized emission spectra for Cu- and Zn-loaded Ru(bpy)$_2$(phen-IA)-azurin. (B) Models of EngT efficiencies based on eq 6 (where τ = 1.67 μs and R_0 = 35.1 Å) and EleT efficiencies based on eq 5 (where τ = 1.67 μs and β = 1.4, 1.2, and 1.0, as shown in legend) for Ru(bpy)$_2$(phen-IA)-azurin.

and Figure S6A) and the nonlinear dependence of the log(k_1) rates versus distance (Figure 3), in addition to the low probability of EleT at longer distances (see Figure 4B and Figure S6B), an EngT mechanism is plausible via photo-induction. If EngT occurs in our azurin model systems, emission associated with the excited-state decay (i.e., Ru^{2+}* to Ru^{2+} transition) quenched by the Cu^{2+} cofactor should be observed. To investigate EngT emission quenching, we conducted time-resolved emission experiments at λ_{em} = 625 nm (λ_{ex} = 490 nm), under conditions matching the transient absorption distance measurements (Figure 5). Time-resolved emission rates for all tested variants are coincidental with the respective transient absorption rates (see Figures 5 and 3, also see Tables S2 and S3). Distinction between EleT and EngT is apparent, considering the significantly different distance dependencies of EleT (eq 3) and EngT (eq 4),

$$k_{EleT}(r) = A \exp[-\beta(r - r_c)] \quad (3)$$

$$k_{EngT}(r) = \frac{1}{\tau_D}\left(\frac{R_0}{r}\right)^6 = k_D\left(\frac{R_0}{r}\right)^6 \quad (4)$$

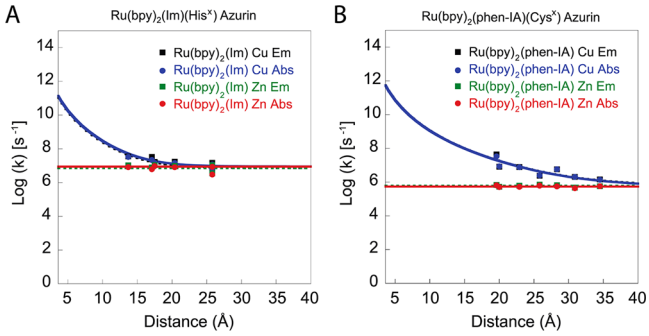

Figure 5. Comparison of photoinduced emission and transient absorption kinetics (both 625 nm), for (A) Ru(bpy)$_2$(Im)-labeled azurin and (B) Ru(bpy)$_2$(phen-IA)-labeled azurin. Blue and red circles and lines are transient absorption data and fits as shown in Figure 4. Cu-metalated and Zn-metalated transient emission data are shown as black, and green squares. Green dashed lines are the average Zn-metalated (unquenched) rates, k_D = 0.599 × 10^6 s^{-1} for Ru(bpy)$_2$(phen-IA)-labeled azurin and k_D = 8.96 × 10^6 s^{-1} for Ru(bpy)$_2$(Im)-labeled azurin. Black dashed lines are the best-fit EngT rate curves (k_{obs}, eq 7), yielding R_0 = 35.1 Å for Ru(bpy)$_2$(phen-IA)-labeled azurin and R_0 = 17.8 Å for Ru(bpy)$_2$(Im)-labeled azurin. Also see Tables S2 and S3.

$$E_{EleT} = \frac{k_{EleT}(r)}{k_D + k_{EleT}(r)} \quad (5)$$

$$E_{EngT} = \frac{k_{EngT}(r)}{k_D + k_{EngT}(r)} \quad (6)$$

$$k_{obs}(r) = k_{EngT}(r) + k_D = k_D\left(\frac{R_0}{r}\right)^6 + k_D \quad (7)$$

where, for EleT (eq 3),[56] r is the center-to-center distance between the donor and acceptor, r_c is the distance of closest approach at molecular contact, and A is assumed to have a value of 10^{13} s^{-1} at $r = r_c$. To match earlier reports, we have assumed r_c = 3.6 Å.[57] β is the exponential coefficient of decay of electronic coupling with r,[57] and values of β for a protein matrix are typically 1.0−1.4 Å^{-1}.[15] For the EngT quenched rate in the presence of an acceptor, $k_{EngT}(r)$ (eq 4),[13,56] τ_D is the donor lifetime in the absence of acceptor, r is the center-to-center distance between the donor and acceptor, R_0 is the Förster distance, and $k_D = 1/\tau_D$ is the donor decay rate in the absence of acceptor. The separate EleT and EngT efficiencies (eqs 5 and 6),[56] which in this simplified form do not take into account both processes occurring concurrently, are the ratios of the decay of interest divided by the sum of the rates of decay of all processes (in both cases including k_D). For EngT, the observed decay rate, $k_{obs}(r)$, in the presence of an acceptor is the sum of the quenched rate, $k_{EngT}(r)$, and the unquenched rate, k_D.[13,56]

Analysis of transient emission data of the Cu-azurin distance variants (Figure 5) yields fits to eq 7, with reasonable Förster radii of 17.8 Å for Ru(bpy)$_2$Im-azurin and 35.1 Å for Ru(bpy)$_2$(phen-IA)-azurin, supporting an EngT mechanism. To demonstrate that the emission decay is coupled to the Cu^{2+} cofactor, we conducted Zn-azurin doping experiments (Figure 6; also see Supporting Information, Figures S7 and S8) using the same step-size used in the transient absorption experiments shown in Figure 4. Consistent with an EngT mechanism, we see a progressive decrease in the amplitudes of the k_1 rates (i.e., for both the Ru(bpy)$_2$Im(His^{83}) and Ru(bpy)$_2$(phen-IA)-

dx.doi.org/10.1021/ja412308r | J. Am. Chem. Soc. 2014, 136, 1793−1802

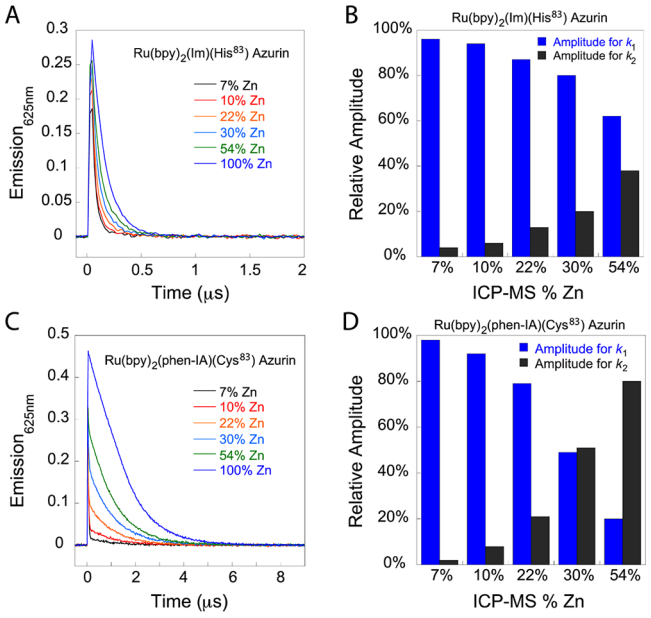

Figure 6. Transient emission kinetics monitored at 625 nm using variable percentages of the Cu- and Zn-metalated forms: (A) $Ru(bpy)_2Im$-(H83) azurin and (C) $Ru(bpy)_2$(phen-IA)-(H83C) azurin. (B) and (D) show relative amplitudes for the k_1 and k_2 rates from global fitting of the 7−54% Zn samples in (A) and (C).

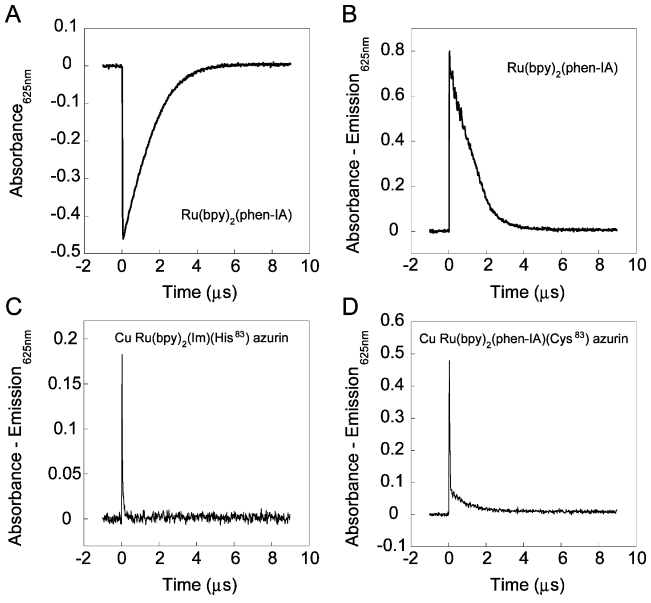

Figure 7. Transient absorption or (absorption − emission) kinetics monitored at 625 nm: (A) $Ru(bpy)_2$(phen-IA) transient absorption, (B) $Ru(bpy)_2$(phen-IA) transient (absorption − emission), (C) Cu-$Ru(bpy)_2Im(His^{83})$ azurin transient (absorption − emission), and (D) Cu-$Ru(bpy)_2$(phen-IA)(Cys^{83}) azurin (absorption − emission). Also see Figure S10.

(Cys^{83}) systems) as the Zn-azurin content increases (Figure 6, also see Table S1). Accordingly, an EngT mechanism is proposed as shown in Scheme 3.

Scheme 3. Putative Energy Transfer Mechanism[a]

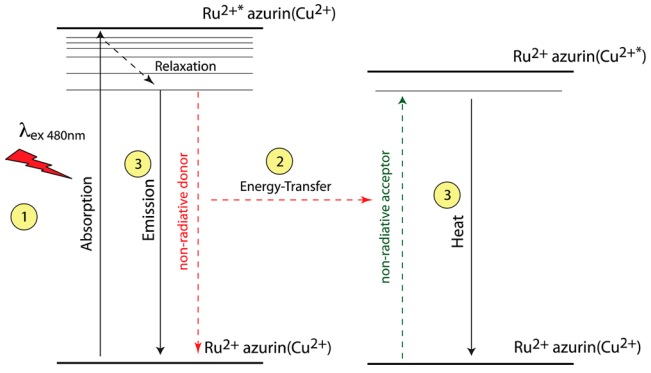

[a](1) laser excitation at 480 nm of Ru^{2+}-azurin/Cu^{2+} results in the formation of the Ru^{2+*}-azurin/Cu^{2+} excited state. (2) Energy transfer from the Ru^{2+*} donor to the azurin/Cu^{2+} acceptor results in the quenching of the observed lifetime of the Ru^{2+*} excited state. (3) Observed emission of Ru^{2+*}-azurin/Cu^{2+} transition to the ground state and the excited Cu^{2+*} acceptor does not re-emit, so return to the Cu^{2+} ground state proceeds by thermal dissipation.

In the proposed EngT mechanism, azurin (Cu^{2+}) is not reduced during the reaction. This implies transient absorption should not be observed, and observed λ_{abs} = 625 nm is actually λ_{em} = 625 nm. To further test this assertion, we conducted transient absorption experiments on the photosensitizers alone (without protein), which clearly illustrates the photon contribution from emission is sufficient to produce erroneous absorption decay (Figure 7A,B). In addition, we conducted transient absorption experiments with Cu-metalated azurin in which the contribution from emission is subtracted from the observed signal (Figure 7C,D, also see Supporting Information, Figure S10). These data suggest the observed decay is dominated by the emission signal, with little, if any, contribution from transient absorption at λ_{abs} = 625 nm.

In principle, we can also experimentally validate the EngT mechanism by monitoring changes in absorption properties associated with the phototrigger upon photoinduction at wavelengths that are remote from the Cu site.[31,33,58] Accordingly, we conducted transient absorption experiments at 310, 370, 432, and 500 nm to demonstrate that $Ru^{3+}(bpy)_2Im(His^{83})$ is not populated and only the $Ru^{2+*}(bpy)_2Im(His^{83})$-to-$Ru^{2+}(bpy)_2Im(His^{83})$ decay is observed. Rates observed at 310 and 370 nm (Figure 8A,B) coincide with those observed at 625 nm (see Table S4 and Table 2). However, there are no observable decays at 432 and 500 nm (Figure 8C,D), which implies that the $Ru^{3+}(bpy)_2Im(His^{83})$ state is not populated.[58] Thus, the observed transient absorption rates at 310 and 370 nm are not likely to be EleT; rather, the observed rates are excited-state decay of the phototrigger (i.e., $Ru^{2+*}(bpy)_2Im(His^{83})$ to $Ru^{2+}(bpy)_2Im(His^{83})$). In other words, these data support an EngT mechanism where the phototrigger decay is quenched by the Cu cofactor (see Table S4). While this observation is in contrast with measurements made by Gray et al.,[25,31,33] it is important to note the transient absorption measurements conducted in these seminal studies were also made via the flash-quench method (Scheme 2B) for $Ru(bpy)_2Im(His^{83})$,[25,31] and the flash-quench method was exclusively used for longer distances.[17] Accordingly, the energy-transfer mechanism proposed in this study (Scheme 3) is not necessarily in conflict with earlier studies; rather, the probabilities of EngT and EleT are nearly equivalent at distances <20 Å (e.g., the $Ru(bpy)_2Im(His^{83})$ system, see Figure S6 and Table S1), and initiating the reaction by prereducing the cofactor (i.e., Cu^{+} azurin) biases

dx.doi.org/10.1021/ja412308r | J. Am. Chem. Soc. 2014, 136, 1793−1802

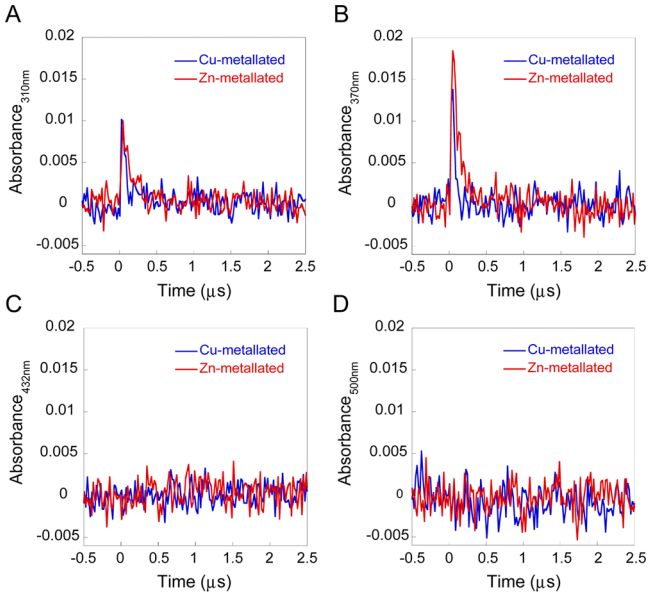

Figure 8. Transient absorption spectra for Cu- and Zn-metalated Ru(bpy)$_2$Im-H83 azurin at (A) 310, (B) 370, (C) 432, and (D) 500 nm. Excitation was at 490 nm for A–C (smaller amplitudes for 310 and 370 nm, but otherwise similar behavior is obtained with excitation at 480 nm). For transient absorption at 500 nm, 480 nm excitation was used to avoid interference from scattered light from the excitation beam. Also see Table S4.

the reaction toward an EleT mechanism upon flash-quench photoinduction (see Scheme 2B).

CONCLUSIONS

The possibility of energy transfer between the excited state of a Ru-polypyridine and the Cu^{2+} site in azurin was not discussed in initial reports[25,30,33] of photoinduced electron transfer and thus was not factored into the construction of the initial putative kinetic mechanism (Scheme 2A). However, more recent reports[31,32] acknowledge the possibility of EngT contributing to the observed photoinduced kinetics but do not resolve the relative contributions of EleT versus EngT. In this study, we present new experimental data that support an EngT mechanism, using methodology (i.e., photoinduction, Scheme 2A) and a protein model system (i.e., azurin Ru(bpy)$_2$Im(His^X)) designed to measure EleT. In addition, we introduce a new azurin model system, Ru(bpy)$_2$(phen-IA)(Cys^X), with a photosensitizer that has a longer lifetime, to accentuate the observed EngT event. To distinguish the two mechanisms, we created distance timetables of transfer rates (Figures 3 and 5), in which there is overlap with putative EleT rates measured previously and distances that approach or exceed the theoretical limits of EleT (Figure 4). It is important to note that the original EleT timetables[17] were reported using data collected via the flash-quench method (Scheme 2B), making EngT quenching unlikely, and the reported data for the photoinduced method (Scheme 2A) were based on a single distance, with proteins labeled at position H83.[25,30−32] In other words, not one of the rates in the timetables reported by Gray et al. is from a measurement of excited-state decay kinetics; i.e., all the azurin rates are from flash-quench generation of Ru^{3+}, and are Cu^{+}-to-Ru^{3+} EleT, where EngT cannot occur (personal communication from H. B. Gray). The photoinduced timetables in this report show a clear divergence away from an EleT mechanism, and these data are best explained by fitting to an EngT model. The critical feature of these data is that, at shorter distances, there is significant overlap between the EngT and EleT rates. In addition, models of both transfer processes show that, at shorter distances, the probabilities of EngT and EleT are nearly coincidental. Accordingly, orthogonal experimental validation is required at shorter transfer distances to distinguish between EleT and EngT, whereas at longer distances the two mechanisms are distinct under photoinduction.

In another important feature of this study, we demonstrate that the lifetime of the excited state of the photosensitizer is coupled to it is proximity to an electron acceptor (i.e., the excited-state decay of the phototrigger is coupled to the Cu^{2+}site, Figure 5). Accordingly, EleT measured at short distances via the photoinduced method has to compete with faster quenching mediated by EngT, reducing the probability of explicit charge transfer, and this is illustrated by the absence of any evidence of the Ru^{3+}(bpy)$_2$Im(His^{83}) state being populated (Figure 8). In initial studies the slower rate k_2 was considered the EleT rate; here we show that sample contaminated with small amounts of Zn-azurin (7%) can produce rates that are on par with putative charge transfer (Table 2). Moreover, the preparation of holo-azurin via enrichment of apo-azurin by way of anion exchange, followed by Cu metalization,[50] or Cu remetalization of apoprotein produced using a strong chelating agent both result in small amounts of Zn-azurin contamination that can only be quantified via extensive metal analysis.

To punctuate this study, we used an alternate cation-exchange chromatography method[38] to isolate 100% Cu-metalated azurin (also see Supplemental Methods and Materials in Supporting Information). In turn, we conducted photoinduced EngT experiments using the Ru(bpy)$_2$Im (His^{83}) system (Figure 9). As expected, the 100% Cu-metalated azurin system is devoid of the minor (slow) kinetic phase observed in the azurin sample contaminated with 7% Zn (see Supporting Information, Figures S4 and S7). In other words, both transient absorption and emission kinetics for the 100% Cu-metalated

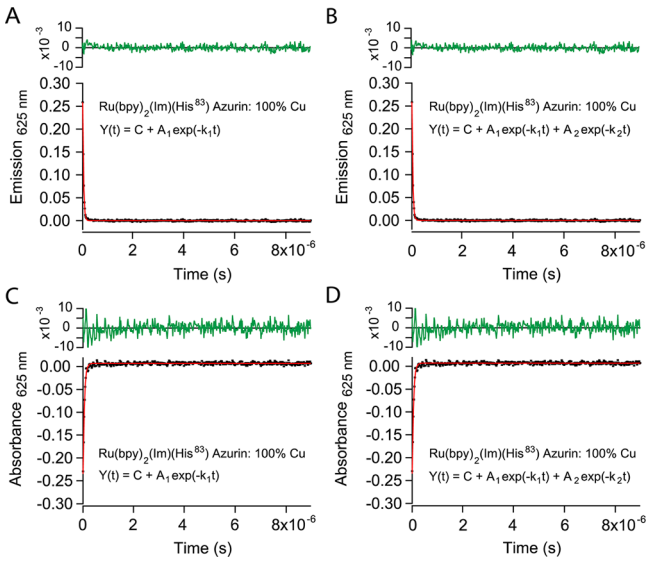

Figure 9. Fits of single exponential, $Y(t) = C + A_1 \exp(-k_1 t)$, and double exponential, $Y(t) = C + A_1 \exp(-k_1 t) + A_2 \exp(-k_2 t)$, functions to 100% Cu (628/280 nm absorbance ratio = 0.60) Ru(bpy)$_2$(Im)-(H^{83}) azurin transient emission (A,B), and transient absorption (C,D) kinetics monitored at 625 nm (λ_{ex} = 490 nm). Also see Table S5.

dx.doi.org/10.1021/ja412308r | J. Am. Chem. Soc. 2014, 136, 1793−1802

$Ru(bpy)_2Im(His^{83})$ system are best fit to a single exponential model with rates that are on par with those reported in our global analysis (in which we extrapolate an expected rate for the pure Cu system; see Table 2 and Supporting Information, Tables S1 and S4). Thus, our proposed EngT mechanism is fully supported, and these experiments completely resolve confounding kinetic phenomena associated with Zn contamination.

In summary, if measurements of electron transfer are conducted via photoinduction, careful quantification of Zn-azurin contamination should be conducted. In addition, independent observation of oxidation of the phototrigger should be conducted along with at least two longer distances to distinguish the two transfer processes. Clear distinction of EngT processes in EleT systems is now of critical importance, in light of the recent ability to confer accelerated EleT via the introduction of electron "hopping" intermediates within a protein matrix.[12]

■ ASSOCIATED CONTENT

Ⓢ Supporting Information

UV−vis spectra of apo and Zn-metalated azurin, correlation of azurin 628/280 nm absorbance ratio to zinc content, cyclic voltammograms, UV−vis spectra, emission spectra, and transfer efficiencies of $Ru(bpy)_2(Im)(His^{83})$ azurin, figures of azurin showing photosensitizer labeling positions, fits to transient absorption and emission data, tables of additional rate data, laser and detector configuration details, and additional Cu-azurin purification protocols. This material is available free of charge via the Internet at http://pubs.acs.org.

■ AUTHOR INFORMATION

Corresponding Author

corey.wilson@yale.edu

Notes

The authors declare no competing financial interest.

■ ACKNOWLEDGMENTS

This work was supported by NSF Award 114846 to C.J.W. We thank Prof. Nilay Hazari for assistance with the synthesis of $Ru(bpy)_2Im$ and $Ru(bpy)_2(phen\text{-}IA)$, and Prof. Zhengrong Wang and Ying Kui for assistance with ICP-MS measurements and analysis. Finally, we thank David N. Beratan and Harry B. Gray for fruitful discussion of this work.

■ REFERENCES

(1) Huber, R. *Angew. Chem., Int. Ed.* **1989**, *28*, 848.
(2) Emerson, R.; Arnold, W. *J. Gen. Physiol.* **1932**, *16*, 191.
(3) Dutton, H. J.; Manning, W. M.; Duggar, B. M. *J. Phys. Chem.* **1943**, *47*, 308.
(4) Arnold, W.; Meek, E. S. *Arch. Biochem. Biophys.* **1956**, *60*, 82.
(5) Karreman, G.; Steele, R. H. *Biochim. Biophys. Acta* **1957**, *25*, 280.
(6) Scholes, G. D. *Annu. Rev. Phys. Chem.* **2003**, *54*, 57.
(7) Winkler, J. R.; Gray, H. B. *Chem. Rev.* **2013**, DOI: 10.1021/cr4004715.
(8) Ceroni, P. *The exploration of supramolecular systems and nanostructures by photochemical techniques*; Springer Verlag: Dordrecht/New York, 2012.
(9) Beljonne, D.; Curutchet, C.; Scholes, G. D.; Silbey, R. J. *J. Phys. Chem. B* **2009**, *113*, 6583.
(10) Gray, H. B.; Winkler, J. R. *Proc. Natl. Acad. Sci. U.S.A.* **2005**, *102*, 3534.
(11) Stubbe, J.; Nocera, D. G.; Yee, C. S.; Chang, M. C. Y. *Chem. Rev.* **2003**, *103*, 2167.
(12) Shih, C.; Museth, A. K.; Abrahamsson, M.; Blanco-Rodriguez, A. M.; Di Bilio, A. J.; Sudhamsu, J.; Crane, B. R.; Ronayne, K. L.; Towrie, M.; Vlcek, A.; Richards, J. H.; Winkler, J. R.; Gray, H. B. *Science* **2008**, *320*, 1760.
(13) Selvin, P. R. *Methods Enzymol.* **1995**, *246*, 300.
(14) Stryer, L. *Annu. Rev. Biochem.* **1978**, *47*, 819.
(15) Gray, H. B.; Winkler, J. R. *Q. Rev. Biophys.* **2003**, *36*, 341.
(16) Farver, O.; Pecht, I. *Coord. Chem. Rev.* **2011**, *255*, 757.
(17) Langen, R.; Chang, I. J.; Germanas, J. P.; Richards, J. H.; Winkler, J. R.; Gray, H. B. *Science* **1995**, *268*, 1733.
(18) Warren, J. J.; Herrera, N.; Hill, M. G.; Winkler, J. R.; Gray, H. B. *J. Am. Chem. Soc.* **2013**, *135*, 11151.
(19) Takematsu, K.; Williamson, H.; Blanco-Rodriguez, A. M.; Sokolova, L.; Nikolovski, P.; Kaiser, J. T.; Towrie, M.; Clark, I. P.; Vlcek, A.; Winkler, J. R.; Gray, H. B. *J. Am. Chem. Soc.* **2013**, *135*, 15515.
(20) Vandekamp, M.; Silvestrini, M. C.; Brunori, M.; Vanbeeumen, J.; Hali, F. C.; Canters, G. W. *Eur. J. Biochem.* **1990**, *194*, 109.
(21) Gunner, M. R.; Dutton, P. L. *J. Am. Chem. Soc.* **1989**, *111*, 3400.
(22) Jeuken, L. J. C.; McEvoy, J. P.; Armstrong, F. A. *J. Phys. Chem. B* **2002**, *106*, 2304.
(23) Monari, S.; Battistuzzi, G.; Bortolotti, C. A.; Yanagisawa, S.; Sato, K.; Li, C.; Salard, I.; Kostrz, D.; Borsari, M.; Ranieri, A.; Dennison, C.; Sola, M. *J. Am. Chem. Soc.* **2012**, *134*, 11848.
(24) Kostic, N. M.; Margalit, R.; Che, C. M.; Gray, H. B. *J. Am. Chem. Soc.* **1983**, *105*, 7765.
(25) DiBilio, A. J.; Hill, M. G.; Bonander, N.; Karlsson, B. G.; Villahermosa, R. M.; Malmstrom, B. G.; Winkler, J. R.; Gray, H. B. *J. Am. Chem. Soc.* **1997**, *119*, 9921.
(26) Prytkova, T. R.; Kurnikov, I. V.; Beratan, D. N. *J. Phys. Chem. B* **2005**, *109*, 1618.
(27) Skourtis, S. S.; Balabin, I. A.; Kawatsu, T.; Beratan, D. N. *Proc. Natl. Acad. Sci. U.S.A.* **2005**, *102*, 3552.
(28) Miller, J. E.; Di Bilio, A. J.; Wehbi, W. A.; Green, M. T.; Museth, A. K.; Richards, J. R.; Winkler, J. R.; Gray, H. B. *Biochim. Biophys. Acta: Bioenergetics* **2004**, *1655*, 59.
(29) Borovok, N.; Kotlyar, A. B.; Pecht, I.; Skov, L. K.; Farver, O. *FEBS Lett.* **1999**, *457*, 277.
(30) Skov, L. K.; Pascher, T.; Winkler, J. R.; Gray, H. B. *J. Am. Chem. Soc.* **1998**, *120*, 1102.
(31) Crane, B. R.; Di Bilio, A. J.; Winkler, J. R.; Gray, H. B. *J. Am. Chem. Soc.* **2001**, *123*, 11623.
(32) Gradinaru, C.; Crane, B. R. *J. Phys. Chem. B* **2006**, *110*, 20073.
(33) Langen, R. Electron transfer in proteins: theory and experiment. Ph.D. Thesis, California Institute of Technology, Division of Chemistry and Chemical Engineering, Pasadena, CA, 1995.
(34) Moser, C. C.; Page, C. C.; Chen, X.; Dutton, P. L. *J. Biol. Inorg. Chem.* **1997**, *2*, 393.
(35) Karlsson, B. G.; Pascher, T.; Nordling, M.; Arvidsson, R. H.; Lundberg, L. G. *FEBS Lett.* **1989**, *246*, 211.
(36) Horton, R. M.; Ho, S. N.; Pullen, J. K.; Hunt, H. D.; Cai, Z. L.; Pease, L. R. *Methods Enzymol.* **1993**, *217*, 270.
(37) Wilson, C. J.; Wittung-Stafshede, P. *Proc. Natl. Acad. Sci. U.S.A.* **2005**, *102*, 3984.
(38) Nar, H.; Huber, R.; Messerschmidt, A.; Filippou, A. C.; Barth, M.; Jaquinod, M.; Vandekamp, M.; Canters, G. W. *Eur. J. Biochem.* **1992**, *205*, 1123.
(39) Lancaster, K. M.; Farver, O.; Wherland, S.; Crane, E. J.; Richards, J. H.; Pecht, I.; Gray, H. B. *J. Am. Chem. Soc.* **2011**, *133*, 4865.
(40) Johnson, E. C.; Sullivan, B. P.; Salmon, D. J.; Adeyemi, S. A.; Meyer, T. J. *Inorg. Chem.* **1978**, *17*, 2211.
(41) Faham, S.; Day, M. W.; Connick, W. B.; Crane, B. R.; Di Bilio, A. J.; Schaefer, W. P.; Rees, D. C.; Gray, H. B. *Acta Crystallogr. D* **1999**, *55*, 379.
(42) Castellano, F. N.; Dattelbaum, J. D.; Lakowicz, J. R. *Anal. Biochem.* **1998**, *255*, 165.

(43) Leckner, J.; Bonander, N.; WittungStafshede, P.; Malmstrom, B. G.; Karlsson, B. G. *Biochim. Biophys. Acta: Protein Struct. Mol. Enzymol.* **1997**, *1342*, 19.
(44) Pace, C. N.; Shaw, K. L. *Proteins* **2000**, 1.
(45) McLaughlin, M. P.; Darrah, T. H.; Holland, P. L. *Inorg. Chem.* **2011**, *50*, 11294.
(46) Jackman, M. P.; Mcginnis, J.; Powls, R.; Salmon, G. A.; Sykes, A. G. *J. Am. Chem. Soc.* **1988**, *110*, 5880.
(47) Zanello, P. *Inorganic electrochemistry: theory, practice and applications*; Royal Society of Chemistry: Cambridge, UK, 2003.
(48) Wilson, C. J.; Wittung-Stafshede, P. *Biochemistry* **2005**, *44*, 10054.
(49) Piccioli, M.; Luchinat, C.; Mizoguchi, T. J.; Ramirez, B. E.; Gray, H. B.; Richards, J. H. *Inorg. Chem.* **1995**, *34*, 737.
(50) McLaughlin, M. P.; Retegan, M.; Bill, E.; Payne, T. M.; Shafaat, H. S.; Pena, S.; Sudhamsu, J.; Ensign, A. A.; Crane, B. R.; Neese, F.; Holland, P. L. *J. Am. Chem. Soc.* **2012**, *134*, 19746.
(51) Jeuken, L. J. C.; Wisson, L. J.; Armstrong, F. A. *Inorg. Chim. Acta* **2002**, *331*, 216.
(52) Monari, S.; Battistuzzi, G.; Dennison, C.; Borsari, M.; Ranieri, A.; Siwek, M. J.; Sola, M. *J. Phys. Chem. C* **2010**, *114*, 22322.
(53) Marshall, N. M.; Garner, D. K.; Wilson, T. D.; Gao, Y. G.; Robinson, H.; Nilges, M. J.; Lu, Y. *Nature* **2009**, *462*, 113.
(54) Chang, I. J.; Gray, H. B.; Winkler, J. R. *J. Am. Chem. Soc.* **1991**, *113*, 7056.
(55) English, A. M.; Lum, V. R.; Delaive, P. J.; Gray, H. B. *J. Am. Chem. Soc.* **1982**, *104*, 870.
(56) Lakowicz, J. R. *Principles of fluorescence spectroscopy*, 3rd ed.; Springer: New York, 2006.
(57) Moser, C. C.; Keske, J. M.; Warncke, K.; Farid, R. S.; Dutton, P. L. *Nature* **1992**, *355*, 796.
(58) Sigfridsson, K.; Sundahl, M.; Bjerrum, M. J.; Hansson, O. *J. Biol. Inorg. Chem.* **1996**, *1*, 405.